



Influence of multidimensional strain-rate effects in eccentrically braced steel frames

Olivier Gauthier Leclerc¹, Charles-Philippe Lamarche², Ouspeha Sin¹

¹ M.A.Sc. Students, Dept. of Civil and Building Engineering, University of Sherbrooke - Sherbrooke, QC, Canada.

² Ph.D., Associate Professor, Dept. of Civil and Building Engineering, University of Sherbrooke - Sherbrooke, QC, Canada.

ABSTRACT

During a severe seismic event, the strain-rates in ductile seismic force resisting systems comprised in steel building structures tend to be high which causes the material to behave differently than when loaded at a slow rate. For this reason, not taking into account strain-rates when designing and/or numerically simulating the response of a structure in such context might lead to erroneous conclusions on the structure's expected behaviour, capacity and expected modes of failure. The present paper presents exploratory dynamic seismic analyses to study the influence of high strain rates on structural steel under a biaxial stress state. These analyses are performed in a practical context through non-linear seismic analyses of a single storey chevron eccentrically braced frame. The complex biaxial nonlinear behaviour of the links in chevron eccentrically braced frame under seismic action is an ideal candidate to study this effect because the deformations in the links occur in both principal directions due to yielding in shear and nonlinear axial deformations induced by bending moments. In the first part of the paper, a nonlinear three-dimensional eccentric link model is calibrated using experimental data found in the literature to make certain that the finite element representation of the link is adequate. Based on the calibrated model, dynamic nonlinear seismic analyses exposed a shear demand increases of 4% in the eccentric link due to high strain rates, confirming the importance to investigate the effect of high strain rates in eccentrically ductile braced frames during seismic events.

INTRODUCTION

Low-rise and mid-rise steel buildings used for light industrial, commercial, and recreational purposes, represent a vast proportion of the building stock in Canada. Most of these buildings are located in regions of active and moderate seismicity levels on the Pacific coast and along the St-Lawrence and Ottawa rivers. For this type of building, the National Building Code of Canada imposes a capacity design philosophy for the design of various seismic force resisting systems (SFRS), for which inelastic response is anticipated under severe dynamic earthquake excitations. During this type of event, the strain-rates in ductile SFRS tend to be high which causes the material to behave differently than when loaded at a slow rate. For this reason, not taking into account strain-rates when designing and/or numerically simulating the response of a structure in such context might lead to erroneous conclusions on the structure's expected behaviour, capacity, and expected modes of failure. The main objectives of the research program that will be only presented in part in this paper is: 1) to characterise the effects of strain-rates on the yield and ultimate stress loci of structural steel (in two dimensions); 2) to develop numerical tools to accurately predict the response of structural elements submitted to complex dynamic inelastic demands; 3) to validate those tools from dynamic test results on eccentrically braced frame links (EBF); and 4), to investigate the effects of strain-rates on current design practices, i.e. to identify the potential changes of failure modes in structures that could lead to a global collapse. Ultimately, the research program aims at: i) better understanding the effects of strain-rates on ductile steel elements; and ii) proposing better seismic design guidelines taking into account the effects of strain-rates. Better designs generally yield to financial economies, but more importantly in safer structures in the event of severe earthquakes.

Many researches were conducted to evaluate the influence of strain-rate on the mechanical properties of structural steel [1], [2], [3], [4]. These studies demonstrated that the main influence of strain-rate on structural steel is the increase of the static yield stress F_y . In the case of a strong seismic event, the range of strain-rate is estimated to lie between 0,25 and 2,5 s⁻¹ [5]. Within this range of strain rates, the dynamic yield stress F_{yd} can increase up to 20% of the static yield stress. Manjoine [6] was one of the first to study the influence of strain-rate on the yield strength and ultimate strength of steel. The tests performed by Manjoine showed an important increase of the yield strength at high strain rates. An increase of lesser importance of the ultimate strength of steel was also observed by Manjoine. In the literature, several strain rate laws are proposed to model the influence of strain-rate on the yield stress. Seven of those models, studied by Sin [7], were compared to uniaxial and biaxial tensile tests performed at various strain rates to characterise the behaviour. The test results are summarized in Figure 1. The test results show that the models proposed by Pan et al. [8], Paul et al. [9] and Rao et al. [3] are those that better predict the

influence of strain-rate on the yield strength in biaxial stress state. The other laws underestimate the increase in yield stress for a value of strain-rate greater than $2 \times 10^{-1} \text{ sec}^{-1}$.

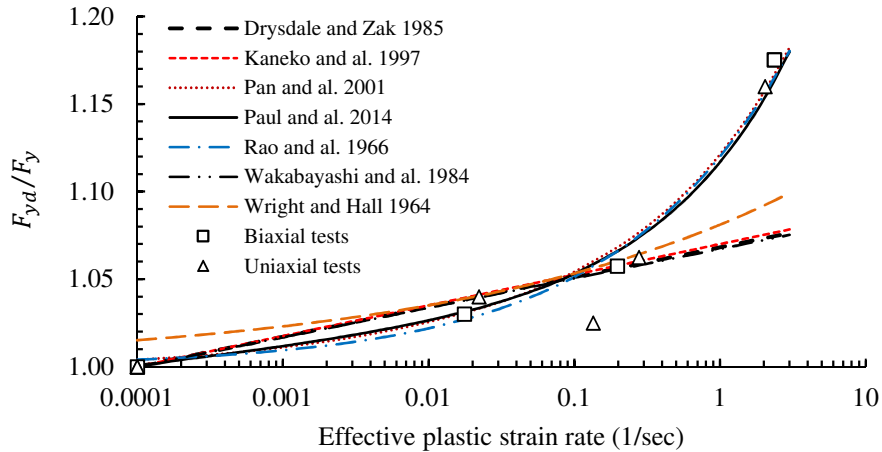


Figure 1. Increase of the yield stress versus the strain-rate according to the seven laws investigated by Sin [7]

In order to study the effect of high strain rates on structural steel under a biaxial solicitation in a practical context, non-linear seismic analyses of a single storey chevron eccentrically braced frame were performed. The complex biaxial nonlinear behaviour of the links in chevron eccentrically braced frame under seismic action is an ideal candidate to study this effect because the deformations in the links occur in both principal directions due to yielding in shear and nonlinear axial deformations induced by bending moments. Before those analyses could be performed with confidence, an eccentric link model was calibrated using experimental data found in the literature.

ECCENTRIC LINK MODEL CALIBRATION

In order to validate the nonlinear behaviour of the finite element model of an eccentric link, the finite element model of an isolated link was calibrated using experimental data. Okazaki and Engelhardt conducted tests on 37 different link specimens with various lengths made of ASTM A992 steel. The experimental test setup is shown in Figure 2. The experimental test setup was made to study the nonlinear cyclic behaviour of eccentric links. Test specimen #9 from Okazaki and Engelhardt [10] was chosen for the calibration of the finite element model. The link is made of a W410x54 and has a length of 1219 mm. Because the link has a length that lie between $1.6M_p/V_p$ and $2.6M_p/V_p$, it is considered to be an intermediate link where the inelastic response is influenced both by shear and flexure. Five intermediate web stiffeners spaced at 203 mm were present on only one side of the web.

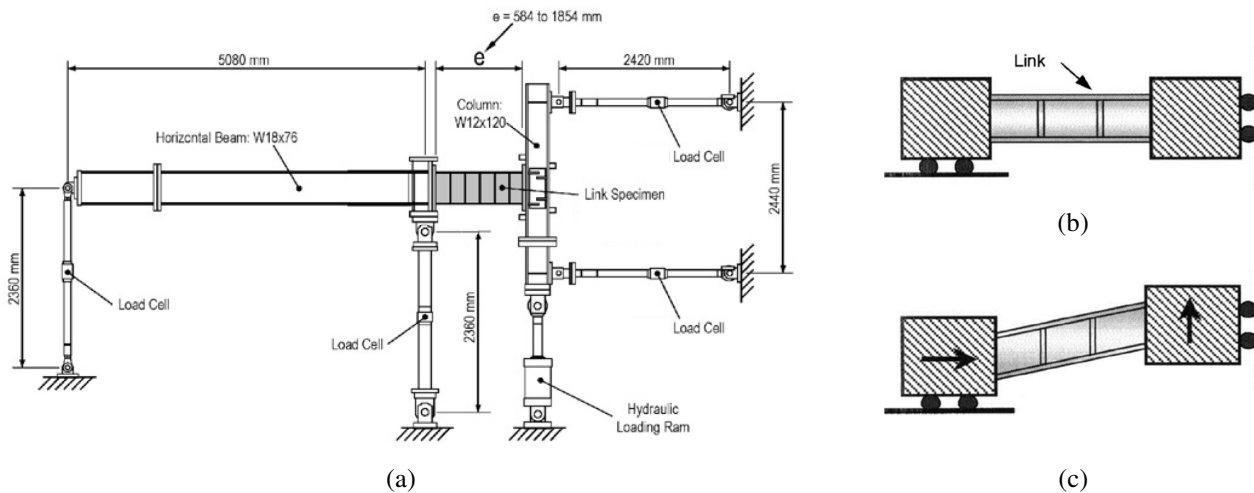


Figure 2. (a) Test set-up (adapted from [10]). Boundary conditions: (b) undeformed link, (c) deformed link (adapted from [11])

Finite element model of the link

The finite element software ADINA was used to model the shear link. The ADINA software provides state-of-the-art capabilities for the stress analysis of solids (2D and 3D) and structures in statics and dynamics. The analysis can be linear or highly nonlinear, including effects of material nonlinearities, large deformations, contact conditions and strain rate effects. The ADINA program offers versatile and generally applicable finite elements for solids, trusses, beams, pipes, plates, shells and gaps. Material models for metals, soils and rocks, plastics, rubber, fabrics, wood, ceramics and concrete are available.

Shell elements with four nodes per element and six degrees of freedom per node were used to model the link. This type of elements was also used by Richards and Uang [11] and Mohebbkhah and Chegeni [12] to model eccentric links and proved to be efficient to predict the strength degradation of a link under reversed cyclic loading. The final choice of the meshing size was established to reach a compromise between the precision of the results and the time needed to complete an analysis. The mesh size of the square elements used is 35 mm by 35 mm. To simulate the boundary conditions on each side of the link corresponding to the experimental test set-up conducted by Okazaki and Engelhardt [10], the boundary conditions shown in Figure 2(a) and Figure 2(b), proposed by Richards and Uang [11], were used. On the right-hand side of the link, only the vertical degree of freedom is free. On the left-hand side of the link, only the degree of freedom in horizontal direction is free. The same cycling loading used in Okazaki and Engelhardt's experiment [10] was imposed to the model. This reverse cyclic rotation history is based on Appendix S of the 2002 AISC Seismic Provisions [13]. The rotation history was imposed to the link by means of an equivalent vertical displacement that is applied at the right end side of the link. The test protocol begins with three cycles of 0.0025, 0.005 and 0.01 rad. Then, the link rotation is increased with 0.01 rad increments every two cycles until a rotation of 0.15 rad is reached.

In order to model the test set-up as accurately as possible, rotational flexibility was introduced on each end of the model presented in Figure 2 using rotational linear spring elements. Six degrees of freedom spring elements were used at each end of the link so that the rotational stiffness can be controlled. The *Rigid links* function available in ADINA was used to constrain the end nodes of the link to the spring element. By using the virtual work method, an estimate of the experimental rotational stiffness of each spring was calculated manually based on the structural elements and the boundary conditions of the test setup. Using these stiffness values as preliminary estimates, the stiffness of the spring elements was varied through multiple simulations until the finite element model compared well with the test results.

Steel material model calibration

Because no cyclic coupon test results were available in Okazaki and Engelhardt [10], the non-linear behaviour of the steel material under cyclic loading was calibrated with experimental data from cyclic coupon test made of A572 steel obtained from Kaufmann [14]. These results were also used as calibration data in other research projects, e.g., Newell and Uang [15], Mojarad and al. [16] and Richards [17]. A nonlinear truss element modelled in ADINA was used to reproduce nonlinear hysteretic behaviour of the steel material provided in Kaufmann [14]. Multiple material models are available in ADINA to model the non-linear behaviour of steel. As a guideline, the plastic-cyclic material model is recommended in the ADINA modeling guide [18]. This material model has proven to produce stable plastic hysteresis under cyclic loading [18]. However, the option of rate-dependent plasticity is not available for this particular model. The only material model in ADINA that can include strain-rate effects in a cyclic loading context is the plastic-multilinear model with isotropic hardening. With an isotropic hardening law, the yield surface of the material will constantly increase under plastic cyclic deformations. In order to better mimic the plastic cyclic behaviour of steel, a maximum yield plateau was set to the ultimate strength of the steel so that the strength of the material does not increase without bound. The ultimate strength of the A572 steel as measured by Kaufmann [14] is 71.9 ksi (496 MPa).

In Figure 3, the results of four simulations using the truss element model are compared to the cyclic coupon tests performed by Kaufmann [14]. The gray curves are the results from Kaufmann. The coloured curves correspond to the simulation results for cyclic tests at 2%, 4%, 6% and 8% strain range levels. These results show that the material model used in the finite element model can predict relatively well the inelastic stress-strain behaviour of structural steel. The typical increase in strength due to the isotropic hardening rule used can be seen in the 2% deformation strain range cycles. It is also clear from Figure 3 that, as expected, the isotropic hardening material model used isn't able to mimic the Bauschinger effect.

Cyclic nonlinear finite element simulation vs test results

To perform the calibration of specimen #9 finite element model, four criteria were considered: the total dissipated energy, the maximum shear demand, the initial shear stiffness and the global aspect of the hysteretic curve. In the case of the elastic shear stiffness, a good approximation of the global stiffness of the experimental setup helped to improve the numerical results. The hysteretic curve corresponding to the total rotation vs the applied shear force of the link of the finite element model and the experimental test are illustrated in Figure 4.

The global shape of the hysteresis obtained from the finite element model matches that of the experimental results quite well. The maximum shear demand value at each cycle is also very similar between the model and the experiment. However, there is a noticeable difference in amplitude for small rotation levels. This can be explained by the behaviour of the steel material model using isotropic hardening where the yield surface expands at each cycle. It is also important to remember that the steel curve used for the material calibration was not taken from Okazaki and Engelhardt experiments. Strength degradation resulting from local buckling of the link's flanges and the web does not occur at the exact same time between the model and the experiment. In the case of the finite element model, strength degradation due to local buckling begins to appear at the 16th loading cycle at a rotation of 0.05 rad compared to the 18th cycle with a rotation of 0.06 rad for the experiment. The dissipated energy and the maximum shear demand values are compared in Table 1.

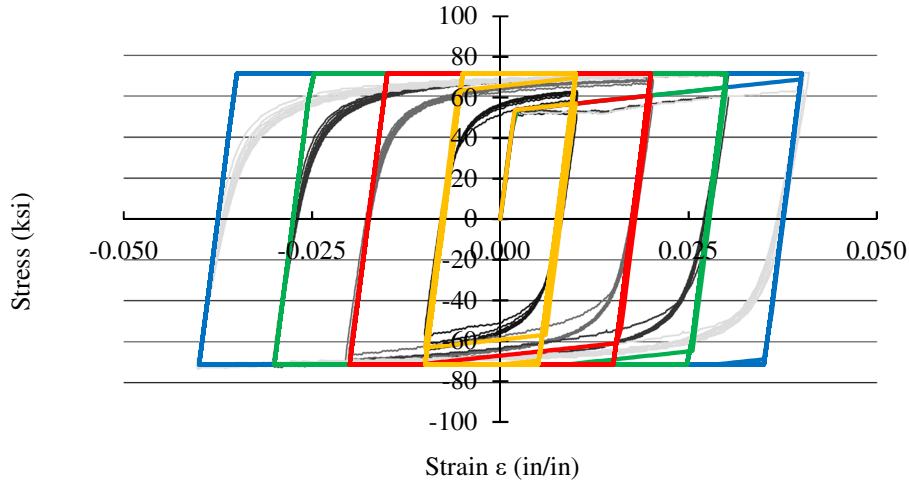


Figure 3. Cyclic strain behavior for 2%, 4%, 6% and 8% strain range using a plastic-multilinear material model

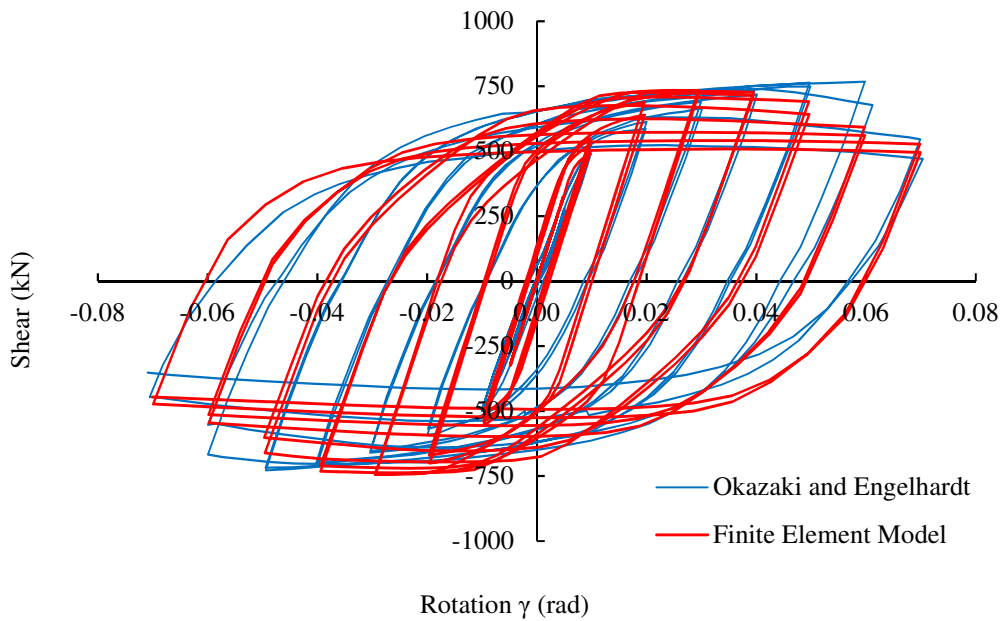


Figure 4. Hysteresis curves of the applied shear versus the total rotation of the link.

Table 1. Dissipated energy and maximum shear demand

	Okazaki and Engelhardt	Finite element model	Difference %
Dissipated Energy (kN-m)	1300	1293	-0,52%
Maximum Shear (kN)	768	744	-3,05%

In the case of the total dissipated energy, a relative difference equal to -0,52% was observed. A relative difference of -3,05% was observed in the case of the maximum shear demand. Figure 5 (a) shows the test specimen after the test [10] and Figure 5(b) shows the finite element model of the specimen after the reverse cyclic protocol. The finite element model was able to reproduce the same failure mode as the one obtained experimentally when the link is submitted to reverse cyclic loading. Large deformations are visible in the end panels where the section is distorted due to combined flange and web buckling.

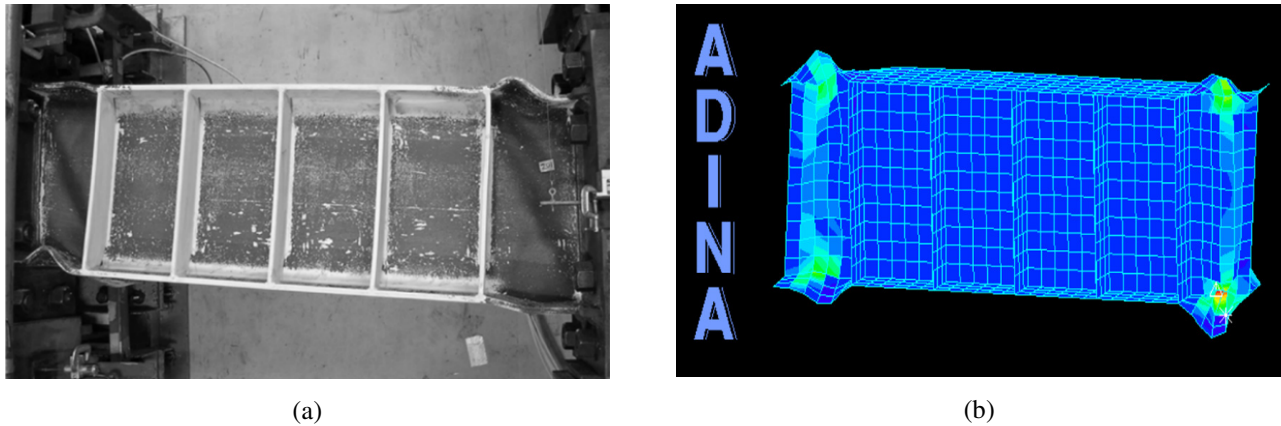


Figure 5. Deformed state at the end of the cyclic loading protocol: (a) experimental test [10], (b) finite element model

EFFECT OF STRAIN RATE ON THE SEISMIC BEHAVIOUR OF AN ECCENTRICALLY BRACED FRAME

Building structure

The building structure studied is the single story Eccentric Braced Frame (EBF) presented in Figure 6(a). The in-plane dimensions of the building were taken as those proposed by [19]. The direction of analysis is the y direction. The two eccentric braced frames depicted graphically in Figure 6(a) have a bay width of $L = 8$ m and the story height is $h_s = 4$ m. The flexibility of the roof diaphragm was not considered in the analyses. The building is assumed to be located in the city of Montreal on a class C soil. The gravity and lateral loads used for the design were calculated according to the 2015 edition of the National Building Code of Canada [20]. The seismic base shear was determined based on the equivalent static force procedure of the NBCC [20]. The ductility-related force reduction factor R_d is equal to 4.0 and the overstrength-related factor R_0 is equal to 1.5. The EBF was sized following capacity design principles in compliance with the clause 27 of the CSA S16-14 [21]. Using this design procedure, the following members were obtained: outer beams: W158x18; braces: HSS152x152x9.5m; columns: W200x36. The link is made of the same member size as the outer beams and is $e = 560$ mm long, therefore, the eV_p/M_p ratio is 2.01, corresponding to an “intermediate link” according to CSA-S16-14. The maximum allowable plastic rotation for this link according to CSA S16-14 is $\gamma_{p,max} = 0.554$ rad.

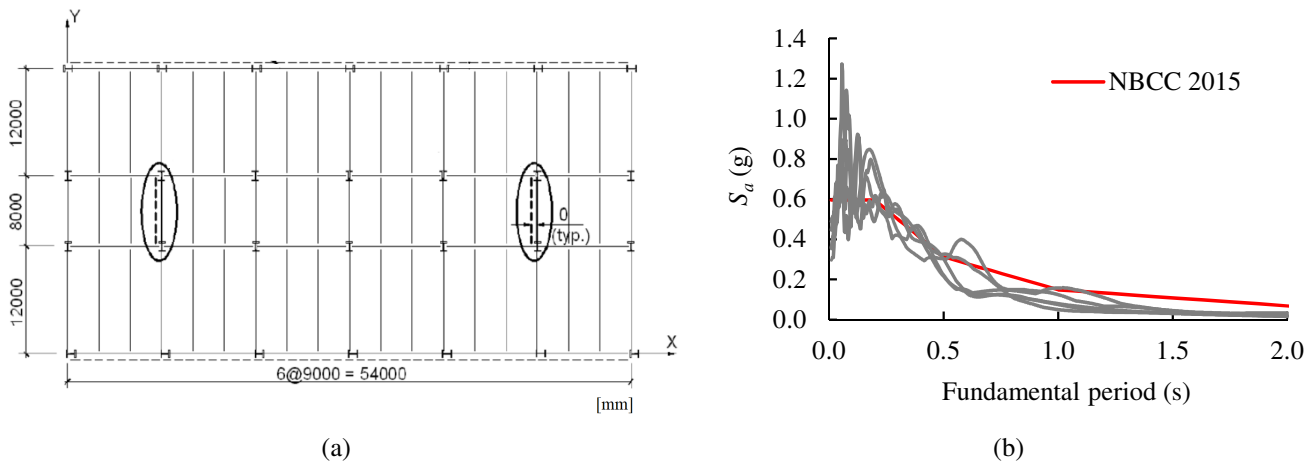


Figure 6. (a) Plan view of the building structure[19]; (b) calibrated earthquake spectrum

Nonlinear dynamic seismic analyses

The eccentric braced frame was modeled with the finite element software ADINA. The gravity columns and beams were not considered in the analyses. The link was modeled in 3D with the same procedure described for the calibration of test specimen #9. The outer beams, braces and columns part of the SFRS were modeled using elastic beam elements. Four seismic masses were concentrated in the horizontal direction at the beam-to-column joints and the beam-to-brace joints. Mass-proportional damping with 3% damping ratio was used. The only rate-dependent material model available in ADINA is the Drysdale and Zak model. This model has been studied by Sin [7] that compared it with experimental results (Figure 1). One of the conclusions of Sin's study was that the Drysdale and Zak model underestimates the increase of the yield strength for strain-rates greater than 0.02 sec^{-1} . Despite this fact, this model was used for the purpose of this exploratory analysis because no other models were available in ADINA.

The seismic design provision of the National Building code of Canada [20] characterises earthquake ground motion levels in term of a uniform hazard spectrum (UHS) having a 2% chance of exceedance in 50 years. The UHS is a function of the fundamental period of a given structure and can be used as a tool to determine the seismic response of a structure in the linear regime. However, for nonlinear analyses, ground motion time histories are needed as inputs to perform dynamic analyses. In this study, the method developed by Atkinson [22] was used to calibrate the earthquake records. The method proposed by Atkinson [22] consists in calibrating synthetic ground motions based on a stochastic method. For a building located in Montreal on a class C soil, Atkinson recommends using records from the east M6 set 1 collection. Because the fundamental period of the eccentric braced frame is equal to $T_a = 0.43 \text{ s}$, the period range used for the calibration lies between 0.1 and 0.5 s. By using the Atkinson's method, a total of five records were chosen and calibrated. The results for a period range from 0 to 2 s are shown in Figure 6(b).

Nonlinear dynamic seismic analyses' results

In total, twenty nonlinear dynamic analyses were performed. First, ten analyses were performed without including the strain rate effects in the model. Out of those ten analyses, five analyses were performed using the design level earthquake accelerograms that were previously scaled. In order to try imposing greater strain rates in the EBF link, the five same simulations were repeated using the same accelerograms with there amplitude doubled. The other ten analyses performed correspond to those previously described, but including the strain rate effects in the model. Figure 7(a) presents the maximum normalized base shear vs story drift hysteretic response obtained from the design earthquake level accelerograms.

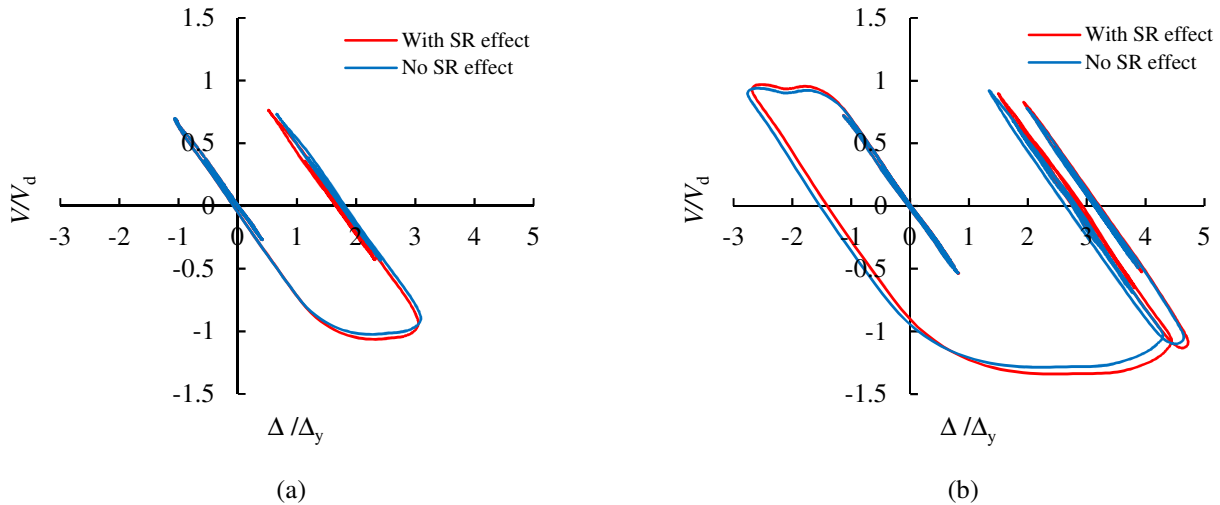


Figure 7. Normalized maximum base shear vs story drift hysteretic response: (a) design level accelerograms; (b) amplified accelerograms (x2)

The maximum story drift caused by the design earthquakes is $0.0052h_s$, which is inferior than the maximum value permitted by the NBCC ($0.025h_s$). This story drift corresponds to a global displacement ductility level of $\Delta/\Delta_y = 3.1$, where $\Delta_y = 6.78 \text{ mm}$ was evaluated from a static push over analysis of the frame. The maximum absolute value of base shear to design base shear ratio V/V_d reached during the analyses is equal to 1.0 when no strain rate effects were included in the models. Figure 7(b) presents the maximum normalized base shear vs story drift hysteretic response obtained from the amplified earthquake level accelerograms. The maximum story drift caused by the amplified earthquakes is $0.008h_s$, corresponding to a global displacement ductility level of $\Delta/\Delta_y = 4.7$. The maximum absolute value of base shear to design base shear ratio V/V_d reached

during the analyses is equal to 1.29 when no strain rate effects were included in the models. As expected, this overstrength value is in line with the maximum probable overstrength prescribed by the CSA S16-14, $R_y = F_u/F_y = 1.3$. The relative increase in base shear due to the effect of high strain rates is 3.8% and 4.2%, for Figure 7(a) and Figure 7(b), respectively. The increase in the shear demand, suggests that the effective global strain rate level would be approximately equal to 0.1 s^{-1} according to Drysdale and Zak law (Figure 1). This strain rate level is consistent with what has been observed by Gioncu (2000). The strain rate levels obtained have yet to be validated by carefully analysing the finite element strain output results. The effect of the strain rate on the shear demand is almost the same from Figure 7(a) and Figure 7(b), even though the amplitude level of the accelerogram was doubled. This is due to the fact that the dynamic yield stress of structural steel is a function on the logarithm of the plastic strain rate level.

Figure 8(a) presents the shear vs total rotation in the link corresponding to the maximum response obtained from seismic analyses using the design level earthquakes, with and without the strain rate effects. Figure 8(b) presents the shear vs total rotation in the link corresponding to the maximum response obtained from seismic analyses using the amplified level earthquakes, with and without the strain rate effects. Because the global behaviour of the frame is governed by the shear deformations in the EBF link, the increase in the maximum shear demand in Figure 8(a) and (b) are the same as those observed in Figure 7. The maximum plastic rotation demand γ_p for the design earthquake level simulation case is 0.040 rad, which is inferior than the maximum value allowed by CSA-S16-14, i.e., $\gamma_{p,max} = 0.0554 \text{ rad}$ for this particular link.

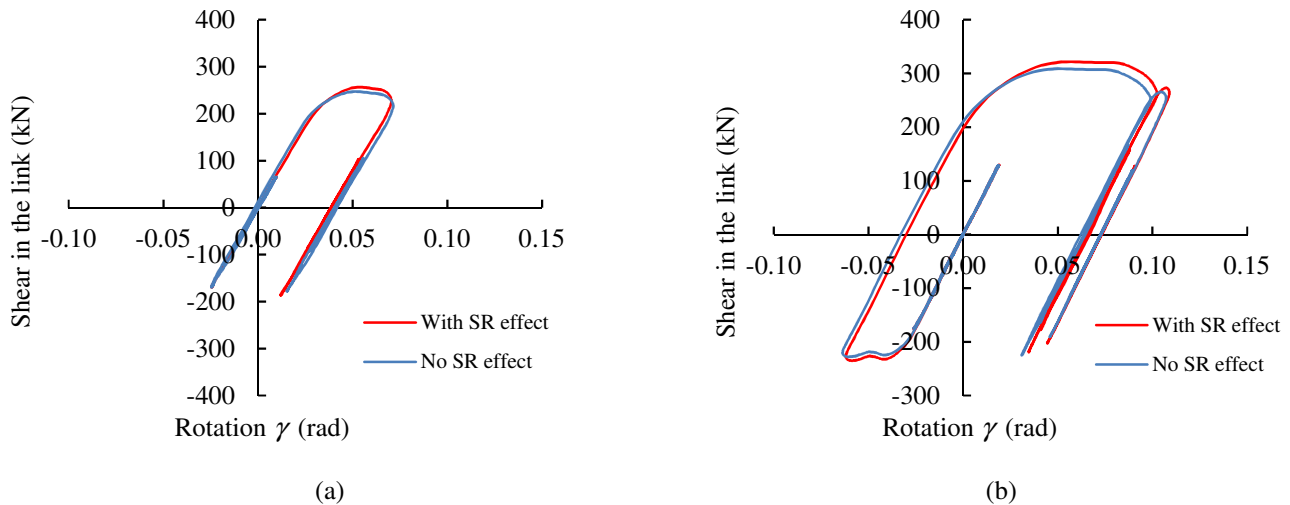


Figure 8. Maximum shear demand in the link versus rotation response: (a) design level accelerograms; (b) amplified accelerograms (x2)

CONCLUSIONS

The paper presented exploratory dynamic seismic analyses to study the influence of high strain rates on structural steel under a biaxial strain solicitation. These analyses were performed in a practical context through non-linear seismic analyses of a single storey chevron eccentrically braced frame. The complex biaxial nonlinear behaviour of the links in chevron eccentrically braced frame under seismic action is an ideal candidate to study this effect because the deformations in the links occur in both principal directions due to yielding in shear and nonlinear axial deformations induced by bending moments. In the first part of the paper, a nonlinear three-dimensional eccentric link model was calibrated using experimental data found in the literature to make sure that the finite element representation of the link is adequate. Based on the calibrated model, dynamic nonlinear seismic analyses exposed a shear demand increases of 4% in the eccentric link due to high strain rates, confirming the importance to investigate the effect of high strain rates in ductile braced frames during seismic events. Though this relative increase is relatively small in the present study, the effect of high strain rates is believed to be more important in multi-story building structures where the effect of higher modes of vibration should greatly amplify the strain rate levels. The next phase of this research project will study this particular aspect.

ACKNOWLEDGMENTS

The financial support from the Fonds de recherche du Québec – Nature et technologies (FRQNT) of the Québec Government, Canada, and the Natural Sciences and Engineering Research Council of Canada (NSERC) is acknowledged.

REFERENCES

- [1] Chang, K., and Lee., G. (1987). "Strain Rate effect on structural steel under cyclic loading". *Journal of Engineering Mechanics*, 1292-1301.
- [2] Nakashima., M. (1988). "Summary report : special theme session on experimental methods for structures. (Part 2 : scale effects in modeling structures) ". *9th World Conf. on Earthquake Engineering*, Tokyo-Kyoto, Japan.
- [3] Rao, N., Tall, L., Lohrmann., M. (1966). "Effect of strain rate on yeild stress of structural steels. *Journal of Materials*, 241.262.
- [4] Wakabayashi, M., Nakamura, T., Yoshida, N., Iwai, S, Watanabe, Y. (1980). "Dynamic loading effetx on the structural performance of concrete and steel materials and beams", in *Proceedings of the 7th World Conference on EarthQuake Engineering*, Istanbul.
- [5] V. Gioncu. (2000). "Influence of strain-rate on the behaviour of steel members". *STESSA 2000 : Behaviour of Steel Structures in Seismic Areas*, Montreal, Canada, p. 19-26.
- [6] Manjoine, J.-M. (1944). "Influence of rate of strain and temperature on yield stress of mild steel". *Journal of Applied Mechanics*, A211-A218.
- [7] Sin, O. (2017) "Étude en deux dimensions de l'effet du taux de déformation sur la limite élastique de l'acier structural". Université de Sherbrooke, Sherbrooke, Canada.
- [8] Pan, L.C., Wu, S., Yu, W. (2001) "Strain rate and aging effect on the mechanical properties of sheet steels". *Thin-Walled Structures*, 429-444.
- [9] Paul, K.S., Raj, A., Biswas, P., Manikandan, G., Verma, R. (2014) "Tensile flow behavior of ultra low carbon, low carbon and micro alloyed steel sheets for auto application under low to intermediate strain rate", *Materials & Design*, 211-217.
- [10] Okazaki, T. and Engelhardt, M. D. (2007) "Cyclic loading behaviour of EBF links constructed of ASTM A992 steel". *Journal of Constructional Research*, 63(6), 751-765.
- [11] Richards P., and Uang, C.-M. (2005). "Effect of Flange Width-Thickness Ratio on Eccentrically Braced Frames Link Cyclic Rotation Capacity". *Journal of Structural Engineering*, 131(10), 1546-1552.
- [12] Mohebkhah, A. and Chegeni, B. (2014). "Overstrength and Rotation Capacity for EBF Links Made of European IPE Sections". *Thin-Walled Structures*, 74, 255-260.
- [13] American Institute of Steel Construction, Inc. (AISC). (2002). "Seismic Provisions for Structural Steel Buildings" Standard ANSI/AISC 341-02, Chicago, Illinois.
- [14] Kaufmann, E.J., Metrovich, B., Pense, A.W. (2001). "Characterization of Cyclic Inelastic Strain Behavior On Properties of A572 Gr. 50 and A913 Gr.50 Rolled Sections". *Advanced Technology for Large Structural Systems*. Report 01-13.
- [15] Newell., J. and Uang, C.-M. (2006). "Cyclic Behavior of Steel Columns With Combined High Axial Load And Drift Demand". University of California, San Diego.
- [16] Mojarad, M., Daei, M., Hejazi, M. (2017) "Optimal Stiffeners Spacing for Intermediate Link in Eccentrically Braced Frame to Increase Energy Dissipation". *AUT Journal of Civil Engineering*, 1(1), 39-44.
- [17] P. W. Richards, "Cyclic Stability and Capacity Design of Steel Eccentrically Braced Frames". University of California, San Diego, 2004.
- [18] ADINA. (2013). *ADINA : Theory and Modeling Guide Volume I*. Watertown, Massachusetts: ADINA R & D, Inc.
- [19] Koboevic, S., Rozon, J., Tremblay, R. (2012) "Seismic Performance of Low-to-Moderate Height Eccentrically Braced Steel Frames Designed for North American Seismic Conditions". *Journal of Structural Eng.*, 138(12), 1465-1476.
- [20] National Research Council – NRC (2015). *National Building Code of Canada*. Prepared by the NRC, Ottawa, ON., Canada.
- [21] Canadian Standard Association - CSA (2014). *CAN/CSA-S16: Design of steel structures*. Prepared by the CSA, Mississauga, ON., Canada.
- [22] Atkinson, G.M. (2009). "Earthquake time histories compatible with the 2005 National building code of Canada uniform hazard spectrum". *Canadian Journal of Civil Engineering*, 36(6), 991-1000.